ORIGINAL RESEARCH

Exosomal miR-136-5p Derived from Anlotinib-Resistant NSCLC Cells Confers Anlotinib Resistance in Non-Small Cell Lung Cancer Through Targeting PPP2R2A

Guoqing Gu[1,]*
Chenxi Hu[1,]*
Kaiyuan Hui[1]
Huiqin Zhang [1]
Ting Chen[1]
Xin Zhang[2]
Xiaodong Jiang[1]

[1]Department of Oncology, The Affiliated Lianyungang Hospital of Xuzhou Medical University, Lianyungang, Jiangsu, 222000, People's Republic of China; [2]Lianyungang Clinical College of Nanjing Medical University, Lianyungang, Jiangsu, People's Republic of China

*These authors contributed equally to this work

Background: Anlotinib resistance is a challenge for advanced non-small cell lung cancer (NSCLC). Understanding the underlying mechanisms against anlotinib resistance is of great importance to improve prognosis and treatment of patients with advanced NSCLC.
Methods: RT-qPCR assay was used to assess the level of miR-136-5p in anlotinib-resistant NSCLC cells and exosomes derived from anlotinib-resistant NSCLC cells. In addition, miR-136-5p level in tumor tissues from patients who exhibited a poor response to anlotinib therapy and patients who were therapy naïve or patients who exhibited a positive response to anlotinib therapy was detected by RT-qPCR assay.
Results: In this study, we found that high levels of plasma exosomal miR-136-5p is correlated with clinically poor anlotinib response. In addition, anlotinib-resistant NSCLC cells promoted parental NSCLC cell proliferation via transferring functional miR-136-5p from anlotinib-resistant NSCLC cells to parental NSCLC cells via exosomes. Moreover, exosomal miR-136-5p could endow NSCLC cells with anlotinib resistance by targeting PPP2R2A, leading to the activation of Akt pathway. Furthermore, miR-136-5p antagomir packaging into anlotinib-resistant NSCLC cell-derived exosomes functionally restored NSCLC cell anlotinib sensitivity in vitro. Animal studies showed that A549/anlotinib cell-derived exosomal miR-136-5p agomir promoted A549 cell anlotinib resistance in vivo.
Conclusion: Collectively, these findings indicated that anlotinib-resistant NSCLC cell-derived exosomal miR-136-5p confers anlotinib resistance in NSCLC cells by targeting PPP2R2A, indicating miR-136-5p may act as a potential biomarker for anlotinib response in NSCLC.
Keywords: advanced non-small cell lung cancer, anlotinib resistance, exosome, microRNA

Introduction

Non-small cell lung cancer (NSCLC) is the most common type of lung cancer.[1,2] In addition, NSCLS is characterized by highly invasive behavior, resistance to chemotherapy and poor prognosis.[3] Despite advances in diagnosis and treatment strategies, the prognosis of NSCLC patients remains unsatisfactory.[4,5] Therefore, deeper investigation into the exploration of novel therapies of NSCLC is particularly important. Anlotinib is an orally administered multikinase inhibitor, which has inhibitory effects on tumor growth and angiogenesis due to the inhibition of vascular endothelial growth factor receptor (VEGFR) 1 to 3, stem cell factor

Correspondence: Xiaodong Jiang
Department of Oncology, The Affiliated Lianyungang Hospital of Xuzhou Medical University, No. 182 Tongguan North Road, Haizhou District, Lianyungang, Jiangsu, 222000, People's Republic of China
Email jxdpaper@163.com

6329

receptor (c-kit), platelet-derived growth factor receptors and fibroblast growth factor receptor 1 to 4.[5] In addition, anlotinib is currently available as third-line regimen for advanced NSCLC patients.[6] Significantly, anlotinib could prolong progression-free survival and overall survival in patients with NSCLC.[6] However, drug resistance in NSCLC is inevitable. Therefore, it is urgent to investigate the underlying mechanisms of anlotinib resistance in patients with NSCLC and explore novel biomarkers to predict anlotinib response.

Exosomes (50–150 nm) are nanosized membrane vesicles that are actively released by a variety of cells and are released into the extracellular milieu.[7,8] In addition, exosomes have been found to be participating in cell-to-cell communication by transmitting many bioactive molecules, such as proteins, lipids, microRNAs (miRNAs).[9,10] Evidence has shown that tumor cell-derived exosomes play an important role in the development of cancer malignancy via regulating drug resistance.[11] However, whether tumor cell-derived exosomes could confer drug resistance in sensitive cells has not been fully investigated.

MiRNAs are a group of noncoding RNA molecules that post-transcriptionally regulate gene expression by interaction with the 3′-UTRs of target mRNAs.[12,13] In addition, miRNAs have shown to play pivotal roles in several biological processes, such as cell proliferation, metastasis and apoptosis.[14] Chen et al found that miR-136 could promote the proliferation and invasion of gastric cancer cells by targeting PTEN.[15] Shen et al reported that overexpression of miR-136 could promote NSCLC cell growth by targeting PPP2R2A.[16] Meanwhile, it has been shown that miRNAs participated in mediating the resistance in human cancers.[17] However, the roles of miR-136-5p in anlotinib resistance in NSCLC are poorly illuminated. Thus, in this study, we aimed to investigate the role of exosomal miR-136 in the regulation of anlotinib resistance of NSCLC.

Materials and Methods
Patient Samples
A total of 15 tumor tissue samples and 15 plasma samples were collected from 5 patients with NSCLC from the Affiliated Lianyungang Hospital of Xuzhou Medical University and Shanghai Cancer Center at different stages, including pre-therapy, positive response to anlotinib therapy, poor response to anlotinib therapy. In addition, the ethical approval was approved by the ethics committee of the Affiliated Lianyungang Hospital of Xuzhou Medical University. All patients had received gene mutation detection. Among 5 patients who received gene mutation detection, 3 cases were identified as EGFR mutation, while no mutation was detected in the other 2 cases. Written informed consent was obtained from all patients. Our research was conducted in accordance with the Declaration of Helsinki.

RNA Sequencing
Exosomes were isolated from plasma samples using the GETTM Exosome Isolation Kit (GeneExosome technologies). After that, total RNA was extracted from exosomes using miRNeasy® Mini kit (Qiagen) according to the manufacturer's protocol. Sequencing libraries were prepared from all samples using QIAseq miRNA Library Kit. After that, the libraries were quantified by Agilent Bioanalyzer 2100 and sequenced by Illumina HiSeq sequencer (Illumina, San Diego, CA, USA). The prepared sequences were then filtered and aligned using Bowtie tool against the human miRNA sequences downloaded from miRbase.

Function Enrichment Analyses
The target genes of differentially expressed miRNAs (DEMs) were subjected to Gene Ontology (GO) enrichment and Kyoto Encyclopedia of Genes and Genomes (KEGG) pathway analyses using the online tool KOBAS.[18]

Cell Culture and Cell Transfection
Human NSCLC cell lines A549 and NCI-H1975 were purchased from American Type Culture Collection. A549/anlotinib and NCI-H1975/anlotinib cells were obtained discontinuously by gradually increasing doses of anlotinib (range from 5 to 80 μM). Briefly, A549 and NCI-H1975 cells were exposed to anlotinib (5 μM), and the medium was changed every day. When the cells were harvested and then re-seeded and cultured in medium with an increase anlotinib concentration. A549/anlotinib and NCI-H1975/anlotinib cells were generated from parental A549 and NCI-H1975 cells by gradually treating them with increasing doses of anlotinib for more than 3 months.

A549, NCI-H1975, A549/anlotinib and NCI-H1975/anlotinib cell lines were cultured in DMEM medium supplemented with 10% FBS, 100 μ/mL penicillin and 0.1 mg/mL streptomycin and maintained in a humidified incubator containing 5% CO_2 at 37°C.

Cells were transfected with miR-136-5p agomir (5'-ACUCCAUUUGUUUUGAUGAUGGA-3'), miR-136-5p antagomir (5'-UCCAUCAUCAAAACAAAUGGAGU -3') and PPP2R2A siRNA1 (5'-GCTCATACATA TCACATCAACTCAA-3') or PPP2R2A siRNA2 (5'-TGCCCTCTGTGATAGACATTCTAAA-3'; Ribobio, Guangzhou, China) using Lipofectamine 2000 transfection reagent according to the manufacturer's protocols.

Cell Counting Kit-8 (CCK-8) Assay

Cell viability was monitored using a CCK-8 assay kit (Dojindo, Kumamoto, Japan). Cells were seeded onto 96-well culture plates at a density of 5×10^3 cells/well and then treated with CCK-8 reagent (10 μL per well). Subsequently, the absorbance was measured by measuring the absorbance at 450 nm in a microplate reader.

Exosome Isolation and Characterization

Exosomes secreted by A549 and A549/anlotinib cells were isolated by using the GETTM Exosome Isolation Kit (GeneExosome technologies). The exosome samples were detected on a ZetaView nanoparticle tracking analysis (NTA) instrument. In addition, exosomes were identified by transmission electron microscopy (TEM) and confirmed by the expression of exosome markers TSG101 and CD81 and endoplasmic reticulum glucose-regulated protein (Grp78).

Exosome Uptake

A549 and A549/anlotinib cell-derived exosomes were labeled with PKH26 dye for 30 min at 37°C to observe the uptake of exosomes in A549 cells. Subsequently, the internalization of exosomes was measured by a confocal microscope. Nuclei were stained by DAPI. PKH26 fluorescence was excited at 551 nm and emitted at 567 nm. Phalloidin fluorescence was excited at 488 nm and emitted at 526 nm. DAPI fluorescence was excited at 405 nm and emitted at 498 nm.

Co-Culture System

Cy3-labeled miR-136-5p was transfected into A549/anlotinib cells. After that, the transfected A549/anlotinib cells were seeded on a Transwell® polyester permeable supports. In addition, A549 cells were plated on the lower chamber. After 24 h of incubation, cells were imaged using a fluorescence microscope (Olympus). Cy3 fluorescence was excited at 551 nm and emitted at 567 nm.

Flow Cytometry Assay

For the cell apoptosis assay, cells were collected and washed twice with cold PBS. After that, cells were incubated with 10 μL of Annexin V-FITC and propidium iodide (PI) for 30 min in darkness. Subsequently, apoptotic cells were assessed by a flow cytometer (BD Biosciences).

For the cell cycle assay, cells were collected and fixed in 70% ethanol for 30 min. After that, cells were treated with RNase A for 20 min at 37°C and then stained for 30 min in darkness with 1 mg/mL PI. Subsequently, cell cycle distribution was assessed using a flow cytometer.

Western Blot Assay

Total protein from NSCLC cells was quantified by the Pierce BCA Protein assay kit. After that, proteins were subjected to 10% SDS-PAGE and then transferred onto PVDF membranes. After blocking with 5% non-fat milk for 1 h, membranes were incubated with primary antibodies against p-Akt (cat. no. ab38449; 1:1000), Akt (cat. no.18785; 1:1000), p-ERK (cat. no. ab201015; 1:1000), ERK (cat. no. ab184699; 1:1000), BCL-2 (cat. no. ab182858; 1:1000), XIAP (cat. no. ab229050; 1:1000), PPP2R2A (cat. no. ab197194; 1:1000), β-actin (cat. no. 6276; 1:1000) at 4°C overnight. Later on, membranes were incubated with the corresponding HRP-labeled goat anti-rabbit secondary antibodies at room temperature for 1 h. Subsequently, protein bands were visualized using a chemiluminescence detection kit (Thermo Fisher Scientific). All antibodies were procured from Abcam (Cambridge, MA).

RT-qPCR Assay

Total RNA was isolated from cells using the TRIpure Total RNA Extraction Reagent. Later on, total RNA was reversely transcribed using EntiLink™ 1st Strand cDNA Synthesis Kit (ELK Biotechnology). After that, real-time PCR was run with StepOne™ Real-Time PCR System and EnTurbo™ SYBR Green PCR SuperMix kit (ELK Biotechnology). U6 was used as an internal reference of miR-136-5p. Fold changes were calculated by using the $2^{-\Delta\Delta CT}$ formula. U6: 5'- CTCGCTTCGGCAGCACAT-3' (F); 5'-AACGCTTCACGAATTTGCGT-3' (R). miR-136-5p: 5'-TCCATTTGTTTTGATGATGGACT-3' (F); 5'-CTCAACTGGTGTCGTGGAGTC-3' (R).

EdU Staining Assay

Cell proliferation was measured by an EdU kit (Cell-Light EdU Apollo567 In Vitro Kit; Ribobio). Cells were

incubated with EdU for 2 h, fixed in 4% paraformaldehyde and permeated with 0.3% TritonX-100 for 15 min. Later on, cells were stained with Apollo dye, and then incubated with Hoechst 33342 for 30 min. Subsequently, EdU-positive cells were captured using a fluorescence microscope. Apollo fluorescence was excited at 550 nm and emitted at 567 nm. DAPI fluorescence was excited at 405 nm and emitted at 498 nm.

Dual-Luciferase Reporter Assay

The wild-type (WT) and mutated (MT) miR-136-5p target in the PPP2R2A 3'-UTR were cloned into the pGL6-miR-based luciferase reporter plasmids. Later on, A549 cells were co-transfected with the above recombinant plasmids and miR-136-5p agomir or its negative control using Lipofectamine 2000 for 48 h. Subsequently, luciferase activity was monitored using the Dual-Luciferase Reporter Assay System (Promega Madison, WI) with renilla luciferase activity as endogenous control.

Animal Study

BALB/c nude mice (4-week-old and 16–20 g in weight) were purchased from the Experimental Animal Center of Soochow University, and animals were maintained following the recommended procedures of National Institutes of Health guide for the care and use of laboratory animals. A549 cells (10^7 cells) were subcutaneously injected into left flank of nude mice. When the tumors reach about 200 mm³, animals were divided randomly into 5 groups: control, PBS + anlotinib treatment, (NSCLC-anlotinib-NC)-Exo + anlotinib treatment, (NSCLC-anlotinib-miR-136-5p agomir)-Exo + anlotinib treatment, or (NSCLC-anlotinib-miR-136-5p antagomir)-Exo + anlotinib treatment groups. After that, PBS, (NSCLC-anlotinib-NC)-Exo, (NSCLC-anlotinib-miR-136-5p agomir)-Exo, or (NSCLC-anlotinib-miR-136-5p antagomir)-Exo were directly injected into the tumors twice a week for 3 weeks. In addition, mice were administered anlotinib (4 mg/kg) by oral gavage for 2 weeks. Tumor volume was calculated every week using the following formula: volume = 0.5 x length × width². Later on, the mice were euthanized at day 21, and the tumors were removed and weighed. The APO-BrdU™ TUNEL Assay Kit was used to evaluate cell apoptosis in tumor tissues. Animal study was approved by the ethics committee of the Affiliated Lianyungang Hospital of Xuzhou Medical University.

Statistical Analysis

Results were all exhibited as the mean ± standard deviation (S.D.). Differences between three or more groups were analyzed by One-way analysis of variance (ANOVA) and Tukey's tests using GraphPad Prism software (version 7.0). Differences between two groups were analyzed by two-tailed Student's t-test. The difference was significant with a value of *P < 0.05. All data were repeated in triplicate.

Results
NSCLC/Anlotinib Cell-Derived Exosomes Increased NSCLC Cell Proliferation and Anlotinib Resistance

To compare the viability between the anlotinib-sensitive and anlotinib-resistant NSCLC cells, A549, A549/anlotinib cells and NCI-H1975, CCK-8 assay was used to detect the viability of NCI-H1975/anlotinib cells that were grown in medium containing with different concentrations of anlotinib for 72 h. As indicated in Figure 1A and B, anlotinib reduced the viability of A549, A549/anlotinib cells, and NCI-H1975, NCI-H1975/anlotinib cells in a dose-dependent manner. In addition, 20 μM anlotinib induced about 74% and 76% growth inhibition of A549 and NCI-H1975 cells, respectively, whereas 20 μM anlotinib induced about 15% and 10% growth inhibition of A549/anlotinib and NCI-H1975/anlotinib cells (Figure 1A and B). These data suggested that A549/anlotinib and NCI-H1975/anlotinib cells were resistant to anlotinib.

Next, we investigated whether functional factors secreted by anlotinib-resistant NSCLC cells could affect the viability of anlotinib-sensitive NSCLC cells. First, A549 and NCI-H1975 cells were cultured in the CM from A549/anlotinib (A549/anlotinib-CM) and NCI-H1975/anlotinib cells (NCI-H1975/anlotinib-CM), respectively. The results of CCK-8 assay showed that A549/anlotinib-CM and NCI-H1975/anlotinib-CM significantly promoted the viability of A549 and NCI-H1975 cells, respectively (Figure 1C). Additionally, cell viability rate was markedly increased in A549 and NCI-H1975 cells grown in A549/anlotinib-CM and NCI-H1975/anlotinib-CM and subsequently treated with anlotinib, compared with A549 and NCI-H1975 cells grown in A549-CM and NCI-H1975-CM, respectively (Figure 1D). These data indicated that anlotinib-resistant NSCLC cells-CM that contained several functional factors could promote NSCLC cell proliferation and anlotinib resistance.
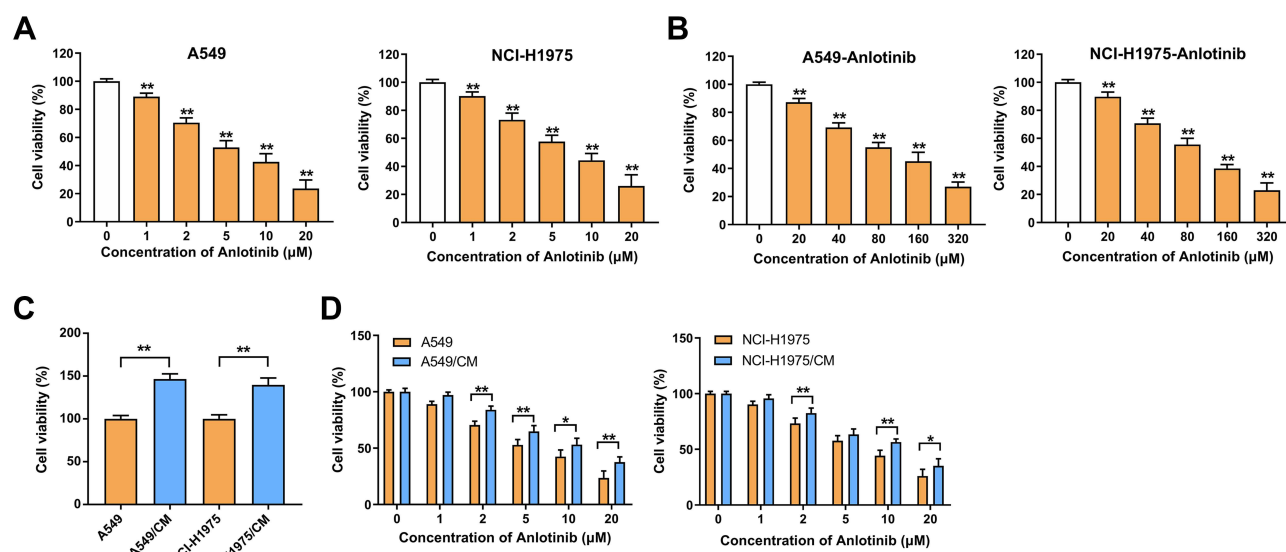
Figure 1 NSCLC/anlotinib cell increased NSCLC cell proliferation and anlotinib resistance. (**A**) CCK-8 assay of A549 or NCI-H1975 cells treated with anlotinib (0, 1, 2, 5, 10 or 20 μM) for 72 h. **P<0.01 compared with 0 μM group. (**B**) CCK-8 assay of A549/anlotinib or NCI-H1975/anlotinib cells treated with anlotinib (0, 20, 40, 80, 160 or 320 μM) for 72 h. **P<0.01 compared with 0 μM group. A549 cells were incubated in A549-CM or A549/anlotinib-CM for 3 days, NCI-H1975 cells were incubated in NCI-H1975-CM or NCI-H1975/anlotinib-CM for 3 days, (**C**) CCK-8 assay was used to determine the viability of A549 and NCI-H1975 cells; (**D**) CCK-8 assays were performed to determine the anlotinib response of these cells. *P<0.05, **P<0.01.

Exosomes are nanoparticles that play an important role in cell-to-cell communication.[19] We have found that anlotinib-resistant NSCLC cells-CM could promote NSCLC cell proliferation and anlotinib resistance. We next investigate whether anlotinib-resistant NSCLC cell-derived exosomes contribute to this effect. Significantly, removing exosomes from A549/anlotinib-CM through ultracentrifugation or inhibiting the exosome secretion of A549/anlotinib-CM through GW4869 suppressed the ability of A549/anlotinib-CM to increase A549 cell viability and anlotinib resistance (Figure 2A). These data showed that A549/anlotinib cell-derived exosomes might play an important role in mediating NSCLC cell proliferation and anlotinib resistance; thus, we isolated exosomes from A549-CM (A549-Exo) and A549/anlotinib-CM (A549/anlotinib-Exo) and confirmed their identity by NTA, TEM and Western blot assays. As shown in Figure 2B and C, A549-Exo and A549/anlotinib-Exo are small nanovesicles from 50 to 150 nm diameter and exhibited typical cup-shaped structures. In addition, the specific surface markers in exosomes, such as TSG101 and CD81, were positively expressed in these vesicles, whereas Grp78 was negative expressed in these vesicles (Figure 2D). Thus, A549-Exo and A549/anlotinib-Exo were isolated successfully.

To assess whether A549-Exo and A549/anlotinib-Exo could be internalized by A549 cells, we labeled A549-Exo and A549/anlotinib-Exo with PKH26 dye and added them into A549 cell culture medium. As revealed in Figure 2E, PKH26 dye was observed in A549 cells, suggesting that A549-Exo and A549/anlotinib-Exo could be internalized by A549 cells. Next, we investigated whether A549/anlotinib-Exo could promote NSCLC cell proliferation and anlotinib resistance. As shown in Figure 2F and G, the results of CCK-8 and flow cytometry assays showed that A549 cells incubated directly with A549/anlotinib-Exo displayed reduced sensitivity to anlotinib. Evidences have shown that Akt and ERK signaling pathways are usually associated with drug resistance of NSCLC cells.[20,21] As indicated in Figure 2H, A549/anlotinib-Exo endowed A549 cells with resistance to anlotinib and activated Akt and ERK signaling. Collectively, A549/anlotinib-Exo could confer anlotinib resistance to A549 cells.

MiR-136-5p is Highly Expressed in Anlotinib-Resistant NSCLC Cells

In an attempt to explore the functional molecules required for the ability of A549/anlotinib-Exo to promote the proliferation and anlotinib resistance in A549 cells, we purified exosomes from plasma samples in patients who exhibited a good response to anlotinib therapy, patients who exhibited a positive response to anlotinib initially and patients who developed a resistance to anlotinib eventually (Table 1). Meanwhile, isolated exosomes were
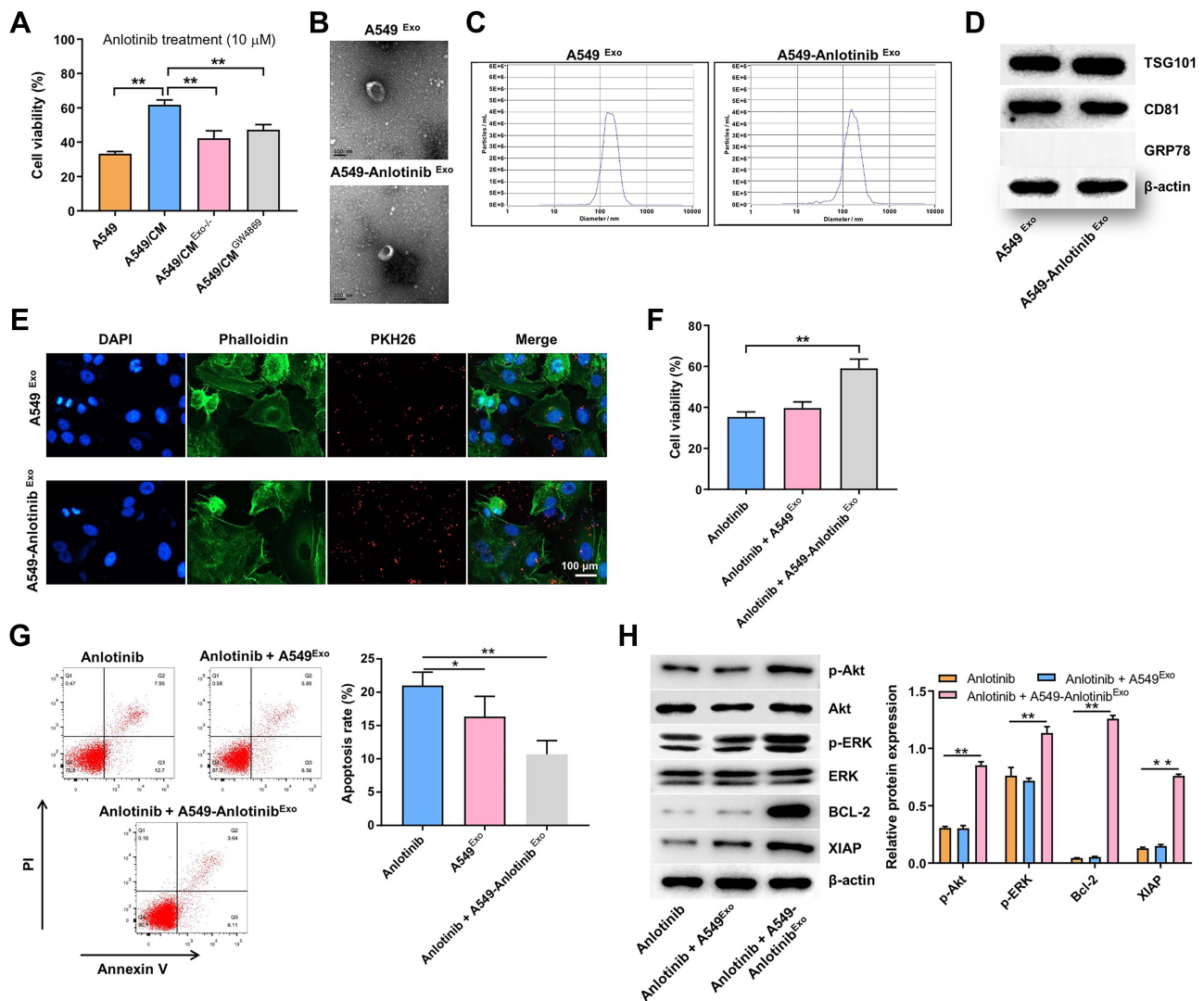
Figure 2 NSCLC/anlotinib cell-derived exosomes increased NSCLC cell proliferation and anlotinib resistance. (**A**) A549 cells were incubated in control-CM, A549/anlotinib-CM, exosome-depleted A549/anlotinib-CM, and A549 cells were co-cultured with GW4869-treated A549/anlotinib cells for 3 days. Cell viability was determined by CCK-8 assay upon anlotinib treatment. **P<0.01. (**B–D**) Identification of exosomes derived from A549 and A549/anlotinib cells by TEM, NTA and Western blot analysis. (**E**) Fluorescent observation of A549 cells after incubation with PKH26-labeled exosomes from A549 or A549/anlotinib cells for 24 h (magnification, ×200). (**F**) A549 cells were incubated with exosomes from A549 (A549[Exo]) or A549/anlotinib cells (A549/anlotinib[Exo]) for 48h, followed by anlotinib treatment for 72 h. Cell viability was measured by CCK-8 assay. **P<0.01. (**G**) Cell apoptosis was measured by flow cytometry assay. *P<0.05, **P<0.01. (**H**) Western blot analysis of p-Akt, Akt, p-ERK, ERK, Bcl-2, XIAP in A549 cells. **P<0.01.

identified by NTA, TEM and Western blot assays (Figure 3A–C). Next, RNA-sequencing was performed to analyze the differentially expressed miRNAs (DEMs) in these isolated exosomes. As shown in Figure 3D and E, 14 upregulated DEMs and 15 downregulated DEMs were detected in exosomes derived from plasma samples in patients with poor anlotinib response relative to patients with good anlotinib response. To gain a more in-depth understanding of the DEMs, the target genes of DEMs were analyzed using GO enrichment and KEGG pathway analyses. GO results indicated that the target genes of DEMs were mainly enriched in the categories "cellular

process", "growth", "molecular transducer activity" and "enzyme regulator activity" (Supplementary Figure 1). As for KEGG pathway analysis, osteoclast differentiation, microRNAs in cancer, tight junction, transcriptional mis-regulation in cancer were mostly associated with the target genes of DEMs (Supplementary Figure 2).

Evidence has shown that miR-136-5p expression is associated with drug resistance in NSCLC.[22] In this study, we found that miR-136-5p levels in tumor tissues and plasma samples were higher in patients who exhibited a poor response to anlotinib therapy compared with patients who were therapy naïve or patients who exhibited

Table 1 Clinical Characteristics of NSCLC Patients in Anlotinib Treatment

	NSCLC Patients (n=15)
Age	
Average	62.6
Range	41–80
Gender	
Male	8 (53.3%)
Female	7 (46.7%)
Histologic type	
Lung adenocarcinoma	14 (93.3%)
Squamous cell lung carcinoma	1 (6.7%)
Fuhrman grade	
III	0 (0%)
IV	15 (100%)
Treatment method before oral treatment with anlotinib	
Radiotherapy	4 (26.7%)
Chemotherapy	10 (66.7%)
Antiangiogenic therapy	2 (13.3%)
Surgery	4 (26.7%)
Tumor targeted therapy	9 (60.0%)

a positive response to anlotinib therapy (Figure 4A and B). Moreover, the level of miR-136-5p is upregulated in A549/anlotinib and NCI-H1975/anlotinib cells compared with that in their parental A549 and NCI-H1975 cells (Figure 4C). Meanwhile, the level of miR-136-5p was higher in the CM of anlotinib-resistant NSCLC cells than that in the CM of NSCLC cells (Figure 4D). Furthermore, high miR-136-5p levels were detected in the serum of mice xenografted with A549/anlotinib cells as well (Figure 4E). These data suggested that miR-136-5p was abundant in anlotinib-resistant NSCLC.

Exosomal Transfer of miR-136-5p from Anlotinib-Resistant NSCLC Cells to NSCLC Cells

We next investigated whether miR-136-5p is responsible for the ability of anlotinib-resistant NSCLC cell-derived exosome to promote parental NSCLC cell proliferation and anlotinib resistance. First, to investigate whether miR-136-5p could be transfer from A549/anlotinib cells to A549 cells via exosomes, A549 cells were grown in A549/anlotinib-CM and exosome-depleted A549/anlotinib-CM, respectively. As indicated in Figure 5A and B, A549 cells cultured in A549/anlotinib-CM expressed a higher level of miR-136-5p than that in A549-CM, whereas the level of miR-136-5p in A549 cells was decreased when exosomes from A549/anlotinib-CM were depleted. Next, A549 cells were indirectly co-cultured
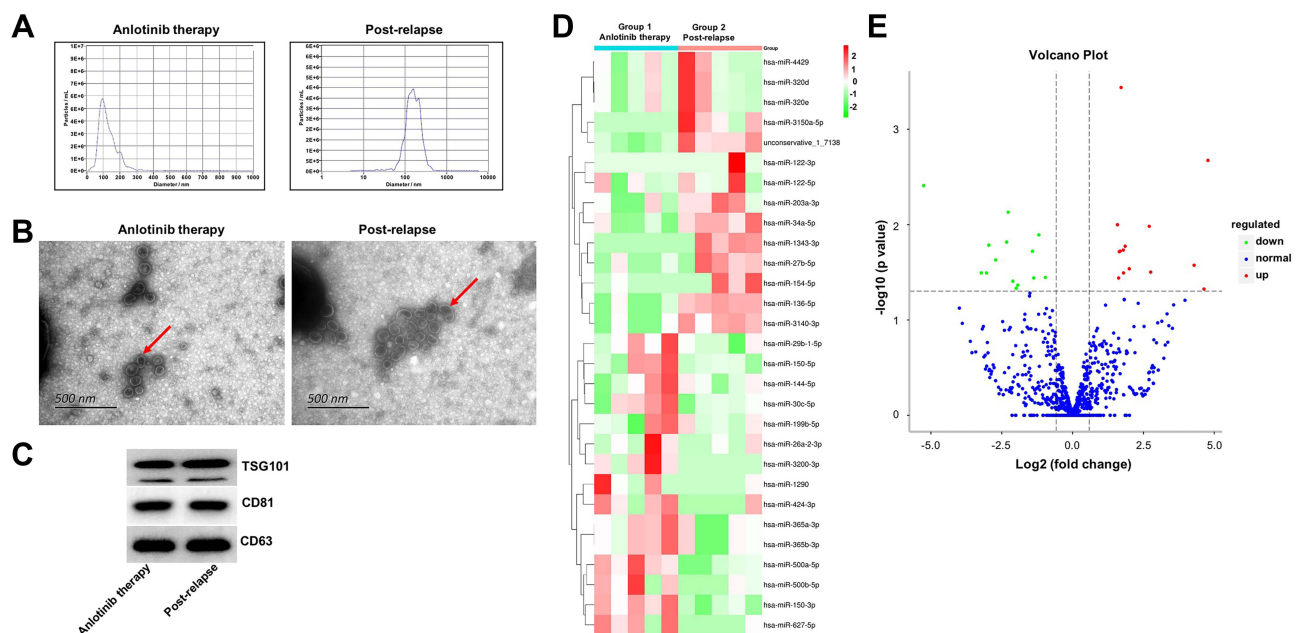

Figure 3 Identification of DEMs. (**A–C**) Exosomes were isolated from plasma samples in patients who exhibited a good response to anlotinib therapy and patients who exhibited a positive response to anlotinib initially and developed a resistance to anlotinib eventually. Exosomes were identified by TEM, NTA and Western blot analysis. The red arrow indicates exosomes. (**D** and **E**) Heat Map and Volcano plot showing the mRNA expression profiles of exosomes that isolated from plasma samples from patients who exhibited a good response to anlotinib therapy and patients who exhibited a positive response to anlotinib initially and developed a resistance to anlotinib eventually.
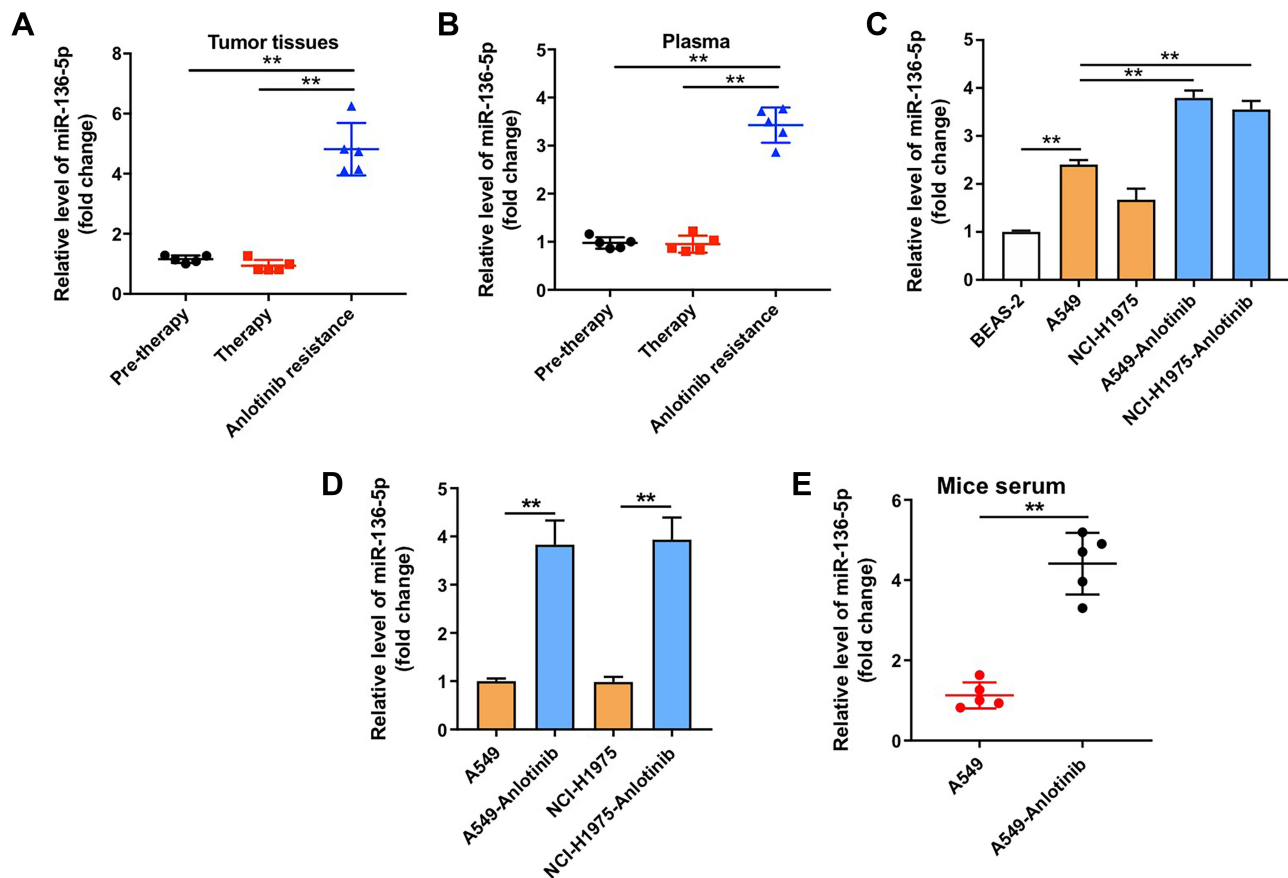
Figure 4 MiR-136-5p is highly expressed in anlotinib-resistant NSCLC cells. (**A** and **B**) RT-qPCR analysis of miR-136-5p level in tumor tissues and plasma from patients who exhibited a poor response to anlotinib therapy and patients who were therapy naïve or patients who exhibited a positive response to anlotinib therapy. (**C**) RT-qPCR analysis of miR-136-5p level in BEAS-2, A549, A549/anlotinib, NCI-H1975 and A549/anlotinib cells. (**D**) RT-qPCR analysis of miR-136-5p level in the CM of anlotinib-resistant and parental cells. (**E**) RT-qPCR analysis of miR-136-5p level in the serum of mice xenografted with anlotinib-resistant and parental A549 cells. **P<0.01.

with A549/anlotinib cells that transiently transfected with Cy3-tagged miR-136-5p. As indicated in Figure 5C, Cy3 fluorescence dye was observed in A549 cells, suggesting that miR-136-5p is contained in A549/anlotinib cell-secreted exosomes and can be transferred into A549 cells. In addition, we further explored the existing pattern of extracellular miR-136-5p. RNase A treatment had very limited effect on miR-136-5p levels in A549/anlotinib-CM; however, RNase A combined with Triton X-100 treatment markedly downregulated miR-136-5p levels in A549/anlotinib-CM (Figure 5D), suggesting that extracellular miR-136-5p was largely encased within the membrane. Meanwhile, miR-136-5p levels were almost equal in whole A549/anlotinib-CM and A549/anlotinib-Exo (Figure 5E).

Additionally, the level of miR-136-5p was upregulated in A549/anlotinib cells transfected with miR-136-5p agomir (A549/anlotinib-miR-136-5p agomir), while miR-136-5p level was downregulated in A549/anlotinib

cells transfected with miR-136-5p antagomir (A549/anlotinib-miR-136-5p antagomir) (Figure 5F). We then isolated exosomes from A549/anlotinib-miR-136-5p agomir-CM (A549/anlotinib-miR-136-5p agomir-Exo) and A549/anlotinib-miR-136-5p antagomir-CM (A549/anlotinib-miR-136-5p antagomir-Exo), respectively, and confirmed their identity by the exosome surface markers TSG101 and CD91 (Figure 5G). Moreover, miR-136-5p level was increased in A549/anlotinib-miR-136-5p agomir-Exo and decreased in A549/anlotinib-miR-136-5p antagomir-Exo (Figure 5H). Functionally, A549 cells incubated with A549/anlotinib-miR-136-5p agomir-Exo displayed reduced sensitivity to anlotinib compared with A549/anlotinib-Exo group, while A549/anlotinib-miR-136-5p antagomir-Exo displayed the opposite results (Figure 5I). Collectively, A549/anlotinib cell-derived functional miR-136-5p could be delivered into A549 cells via exosomes.
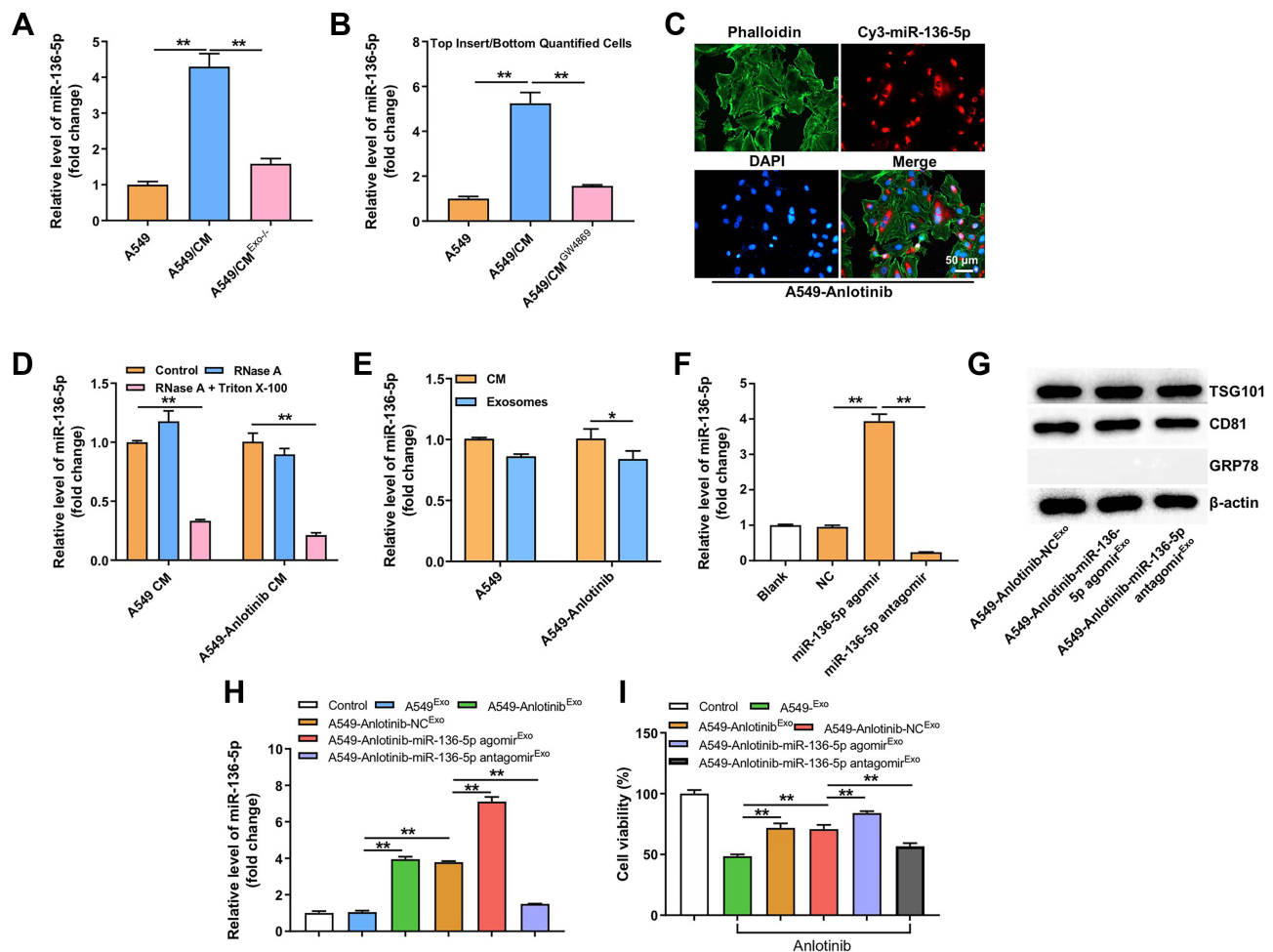
Figure 5 Exosomal transfer of miR-136-5p from anlotinib-resistant NSCLC cells to NSCLC cells. (**A**) RT-qPCR analysis of miR-136-5p level in A549 cells incubated with control-CM, A549/anlotinib-CM, exosome-depleted A549/anlotinib-CM. (**B**) RT-qPCR analysis of miR-136-5p level in A549 cells co-cultured with A549, A549/anlotinib and GW4869-treated A549/anlotinib cells. (**C**) A549/anlotinib cells transfected with Cy3-tagged miR-136-5p were co-cultured with A549 cells for 48 h, and the fluorescence signal was detected by microscopy (magnification, ×200). (**D**) RT-qPCR analysis of miR-136-5p level in the CM of A549 and A549/anlotinib cells treated with RNase A (2 mg/mL) alone or combined with Triton X-100 (0.1%) for 20 min. (**E**) RT-qPCR analysis of miR-136-5p level in A549-CM and A549/anlotinib cell-CM, A549-Exo and A549/anlotinib-Exo. (**F**) RT-qPCR analysis of miR-136-5p level in A549/anlotinib cells transfected with NC, miR-136-5p agomir and miR-136-5p antagomir. (**G**) Identification of exosomes derived from transfected A549/anlotinib cells by Western blot analysis. (**H**) RT-qPCR analysis of miR-136-5p level in A549 cells after incubation with indicated exosomes. (**I**) CCK-8 assay of A549 cells pre-incubated with indicated exosomes for 48 h, followed by anlotinib treatment for 72 h. *P<0.05, **P<0.01.

MiR-136-5p Promoted A549 Cell Proliferation and Anlotinib Resistance

Having demonstrated that A549 cells could uptake A549/anlotinib cell-derived exosomal miR-136-5p, we then investigated whether miR-136-5p could confer anlotinib resistance in NSCLC cells. MiR-136-5p agomir obviously increased the proliferation of A549 cells, while miR-136-5p antagomir markedly inhibited cell proliferation (Figure 6A). In addition, CCK-8, EdU staining assays showed that miR-136-5p agomir obviously promoted A549 cell proliferation and anlotinib resistance; however, miR-136-5p antagomir notably reduced A549 cell proliferation and anlotinib resistance (Figure 6B and C). Moreover, miR-136-5p agomir significantly inhibited anlotinib-induced

apoptosis in A549 cells, whereas miR-136-5p antagomir displayed the opposite results (Figure 6D). Meanwhile, anlotinib notably induced cell cycle arrest at the G0-G1 phase in A549 cells (Figure 6E). However, miR-136-5p agomir remarkably inhibited anlotinib-induced cell cycle arrest in A549 cells, whereas miR-136-5p antagomir displayed the opposite results (Figure 6E). Collectively, miR-136-5p could promote A549 cell proliferation and anlotinib resistance.

PPP2R2A is a Direct Target of Exosomal miR-136-5p in NSCLC

The data in online bioinformatics tool TargetScan showed that PPP2R2A might be a potential target of miR-136-5p (Figure 7A). In addition, the results of dual-luciferase
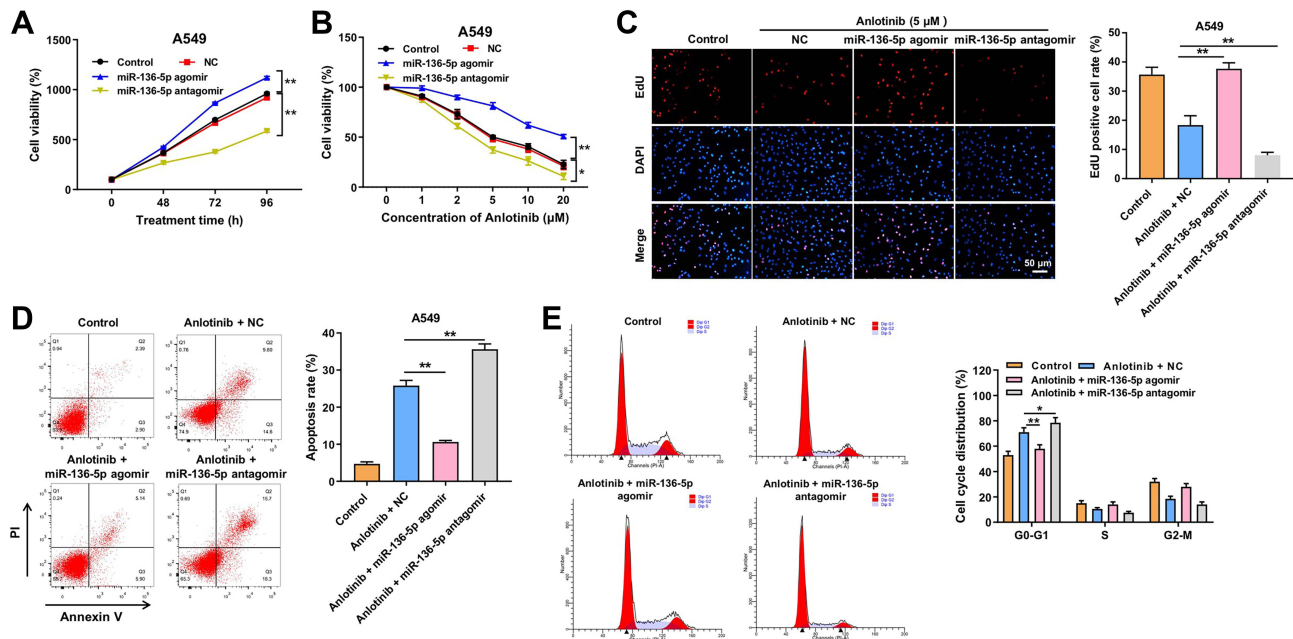
Figure 6 MiR-136-5p promoted A549 cell proliferation and anlotinib resistance. (**A**) CCK-8 assay of A549 cells treated with miR-136-5p agomir or miR-136-5p antagomir for 0, 48, 72 and 96 h. (**B**) A549 cells were treated with miR-136-5p agomir and antagomir for 48 h, followed by anlotinib treatment for 72 h. CCK-8 assay was used to assess cell viability. (**C**) EdU staining assay was used to assess cell proliferation (magnification, ×200). (**D** and **E**) Cell apoptosis and cell cycle distribution were determined by flow cytometry assay. *P<0.05, **P<0.01.

reporter assay showed that the luciferase activity of 3′ UTR of PPP2R2A was suppressed by miR-136-5p agomir, suggesting that miR-136-5p could specifically bind to PPP2R2A (Figure 7B). Moreover, miR-136-5p agomir markedly downregulated the expression of PPP2R2A in A549 cells, whereas miR-136-5p antagomir displayed the opposite results (Figure 7C). Remarkedly, A549/anlotinib-Exo decreased the expression of PPP2R2A in A549 cells as well (Figure 7C). These results indicated that PPP2R2A was a direct target of exosomal miR-136-5p in NSCLC.

MiR-136-5p Promoted A549 Cell Proliferation and Anlotinib Resistance via Downregulation of PPP2R2A

To investigate the functional role of PPP2R2A in miR-136-5p mediated anlotinib resistance in NSCLC cells, A549 cells were transfected with PPP2R2A siRNA1 and PPP2R2A siRNA2. As shown in Figure 7D, PPP2R2A siRNA2 remarkedly reduced the expression of PPP2R2A in A549 cells. Additionally, PPP2R2A siRNA2 significantly decreased the expression of PPP2R2A and increased the expressions of p-Akt, Bcl-2 and XIAP in anlotinib-treated A549 cells (Figure 7E). Moreover, the results of CCK-8 assay showed that PPP2R2A siRNA2 markedly promoted A549 cell proliferation and anlotinib

resistance (Figure 7F). Meanwhile, A549 cells transfected with miR-136-5p antagomir displayed increased sensitivity to anlotinib, which could be abolished by PPP2R2A siRNA2 (Figure 7G). Furthermore, miR-136-5p antagomir enhanced the sensitivity of A549 cells to anlotinib via upregulation of PPP2R2A and downregulation of p-Akt, Bcl-2 and XIAP, whereas PPP2R2A downregulation in A549 cells abolished this effect (Figure 7H). To sum up, miR-136-5p could promote A549 cell proliferation and anlotinib resistance via downregulation of PPP2R2A.

A549/Anlotinib Cell-Derived Exosomal miR-136-5p Agomir Promoted A549 Cell Anlotinib Resistance in vivo

To assess the effect of exosomal miR-136-5p on anlotinib response in vivo, we administered A549/anlotinib-Exo intratumorally into A549 xenografts. As shown in Figure 8A–C, A549/anlotinib-Exo or A549/anlotinib-miR-136-5p agomir-Exo remarkedly dampened the response of A549 xenografts to anlotinib, accompanied by upregulated miR-136-5p level in tumor tissues. In addition, A549/anlotinib-miR-136-5p agomir-Exo suppressed cell apoptosis in xenograft tumors upon anlotinib treatment, whereas A549/anlotinib-miR-136-5p antagomir-Exo displayed the opposite results (Figure 8D). Meanwhile, exosomal miR-
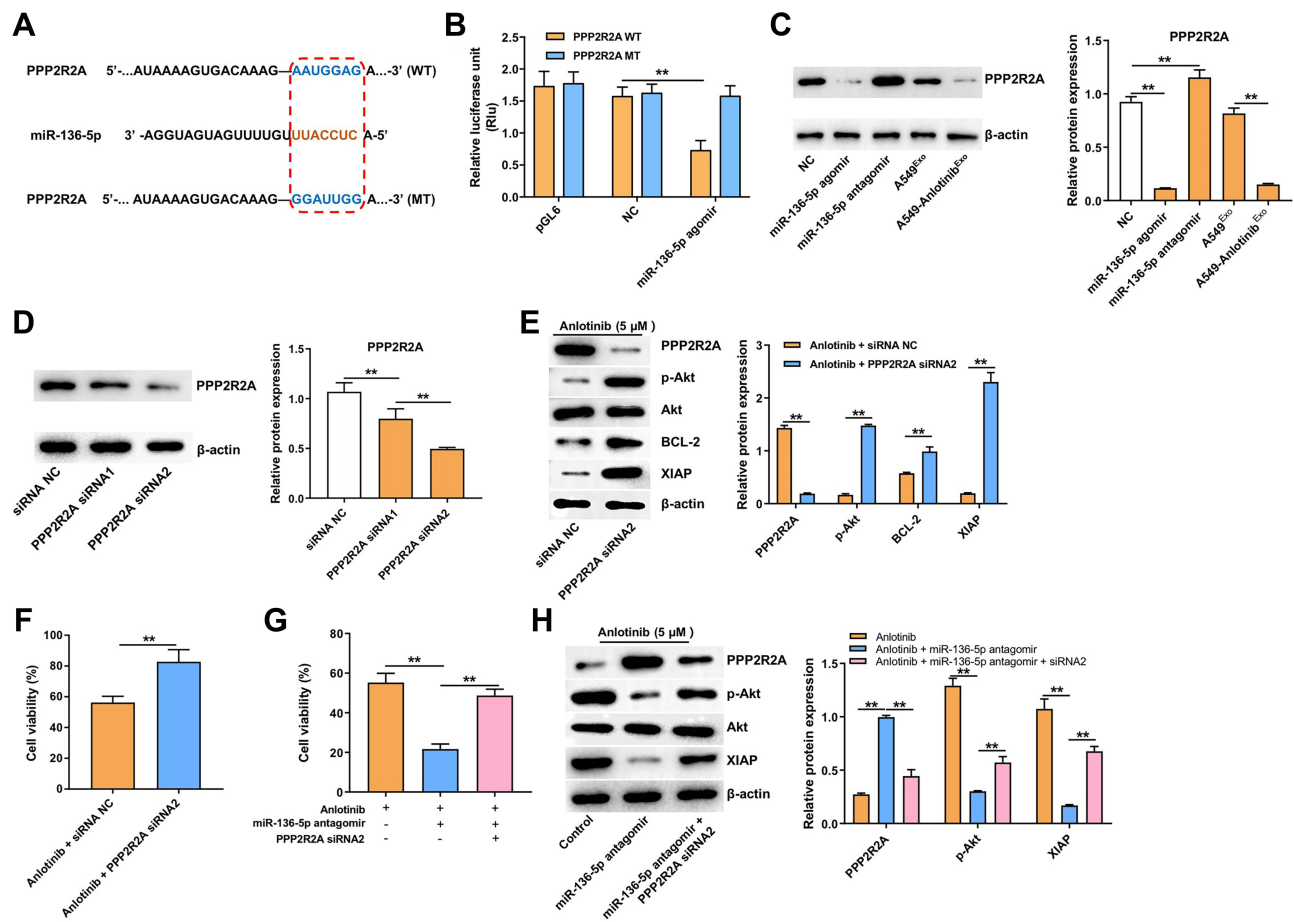
Figure 7 MiR-136-5p promoted A549 cell proliferation and anlotinib resistance via downregulation of PPP2R2A. (**A**) Schematic diagram of binding sites between miR-136-5p and PPP2R2A. (**B**) Luciferase reporter assay validated the relationship between miR-136-5p and PPP2R2A. (**C**) Western blot analysis of PPP2R2A expression in A549 cells treated with miR-136-5p agomir, miR-136-5p antagomir, A549-Exo and A549/anlotinib-Exo. (**D**) Western blot analysis of PPP2R2A expression in A549 cells transfected with PPP2R2A siRNA1 and siRNA2. (**E**) Western blot analysis of PPP2R2A, p-Akt, Akt, Bcl-2 and XIAP expressions in A549 cells transfected with PPP2R2A siRNA2, followed by anlotinib treatment. (**F**) CCK-8 assay of A549 cells transfected with PPP2R2A siRNA2, followed by anlotinib treatment. (**G**) Western blot analysis of PPP2R2A, p-Akt, Akt, Bcl-2 and XIAP expressions in A549 cells transfected with miR-136-5p antagomir or miR-136-5p antagomir plus PPP2R2A siRNA2, followed by anlotinib treatment. (**H**) CCK-8 assay of A549 cells transfected with miR-136-5p antagomir or miR-136-5p antagomir plus PPP2R2A siRNA2, followed by anlotinib treatment. **$**P<0.01$.

136-5p notably decreased the expression of PPP2R2A and increased the expression of p-Akt in xenograft tumors upon anlotinib treatment, whereas A549/anlotinib-miR-136-5p antagomir-Exo displayed the opposite results (Figure 8E). These data indicated that A549/anlotinib cell-derived exosomal miR-136-5p promoted A549 cell anlotinib resistance in vivo via downregulation of PPP2R2A.

Discussion

The response of patients with advanced NSCLC to chemotherapy is poor, owing to intrinsic and acquired chemoresistance.[23–25] At present, anlotinib is used for the third-line treatment of patients with advanced NSCLC.[26] However, acquired resistance to anlotinib has been observed in the clinic in patients with advanced NSCLC.[26] Thus, it is necessary to investigate the

molecular mechanisms underlying anlotinib resistance and identify potential targets for anlotinib-resistance therapy. In the present study, we found that miR-136-5p is highly expressed in anlotinib-resistant NSCLC cells. In addition, overexpression of miR-136-5p promoted anlotinib-resistance by targeting PPP2R2A, leading to the activation of Akt pathway. Moreover, miR-136-5p could be transferred from anlotinib-resistant NSCLC cells to anlotinib-sensitive NSCLC cells via exosomes, transforming anlotinib-sensitive cells into resistant cells, thereby disseminating anlotinib resistance.

Illuminating the molecular mechanisms of anlotinib resistance could contribute to the development of combination therapies to overcome anlotinib resistance. Evidences have shown that exosomes play an important role in chemoresistance in NSCLC.[27] In addition, tumor-
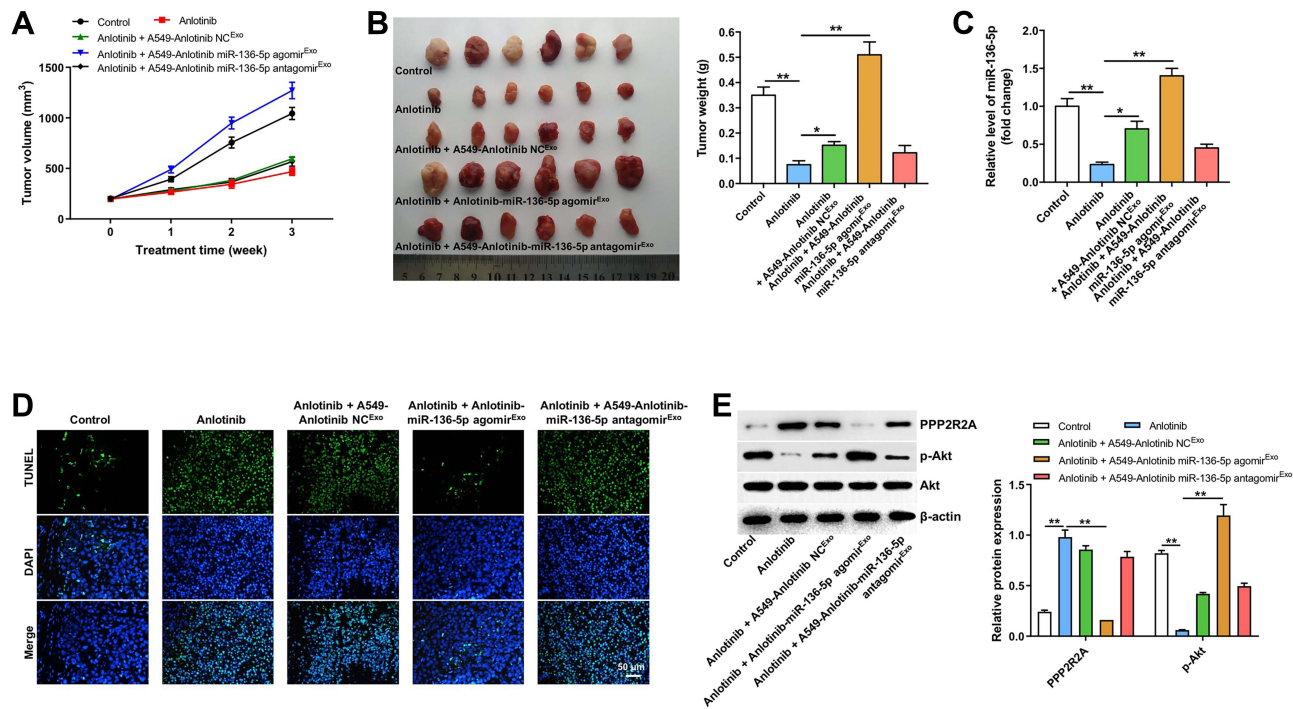
Figure 8 A549/anlotinib cell-derived exosomal miR-136-5p promoted A549 cell anlotinib resistance in vivo. (**A**) Tumor volume was measured. (**B**) Representative image of xenograft tumors and tumor weights. (**C**) RT-qPCR analysis of miR-136-5p level in tumor tissues. (**D**) Cell apoptosis in tumor tissues was assess using TUNEL assay (magnification, ×200). (**E**) Western blot analysis of PPP2R2A, p-Akt, Akt expressions in tumor tissues. *P<0.05, **P<0.01.

derived exosome can deliver various drug resistance-associated miRNAs to recipient cells.[28] Thus, in this study, we performed RNA-sequencing assay to identify the DEMs in exosomes that isolated from plasma samples from patients with good anlotinib response and patients with poor anlotinib response. We found that miR-136-5p level was upregulated in exosomes-derived from plasma samples in patients who exhibited a poor response to anlotinib therapy. In addition, the level of miR-136-5p is increased in anlotinib-resistant NSCLC cells, as well as in the plasma of mice xenografted with A549/anlotinib cells. Therefore, exosomal miR-136-5p might be play an important role in anlotinib resistance.

It has been shown that secreted exosomes loaded with miRNAs could modulate cell biological function and cell signaling in recipient cells.[29,30] Fan et al showed that exosomal miR-210 derived from lung cancer cells could promote the fibroblasts transferring into cancer-associated fibroblasts.[31] Kim et al found that NSCLC cell-derived exosomal miR-619-5p could promote tumor angiogenesis and metastasis by targeting RCAN1.4.[32] Importantly, exosomal miRNAs may play a vital role in mediating resistance transfer from tumor drug-resistant cells to tumor cells.[33] In addition, the ability of exosomal miRNAs

released by drug-resistant tumor cells to transfer the resistant phenotype to sensitive cells has been recognized as a key mechanism for dissemination of drug resistance.[34] In this study, we found that miR-136-5p could be transferred from anlotinib-resistant NSCLC cells to anlotinib-sensitive NSCLC cells via exosomes. In addition, anlotinib-resistant NSCLC cell-derived exosomal miR-136-5p could confer the resistant phenotype to anlotinib-sensitive NSCLC cells. Furthermore, overexpression of miR-136-5p could promote the proliferation and suppress the apoptosis of anlotinib-sensitive NSCLC cells upon anlotinib treatment, whereas downregulation of miR-136-5p suppressed the proliferation and induced the apoptosis of anlotinib-sensitive NSCLC cells upon anlotinib treatment. These data suggested that exosomal miR-136-5p could promote A549 cell proliferation and anlotinib resistance.

Next, we found that PPP2R2A was a binding target of miR-136-5p, which could be inversely regulated by miR-136-5p. PPP2R2A is considered as a tumor suppressor in human cancers.[35,36] Yu et al reported that overexpression of miR-221 could promote osteosarcoma cell proliferation and cisplatin resistance via downregulation of PPP2R2A.[37] Zhang et al found that miR-136 could promote the proliferation of vascular muscle cells in

atherosclerosis via targeting PPP2R2A.[38] Meanwhile, Zhang et al reported that miR-136 could inhibit TGF-β-induced proliferation arrest via downregulation of PPP2R2A.[39] Shen et showed that miR-136-5p could promote the proliferation of NSCLC cells via downregulation of PPP2R2A, which was consistent with our results.[16] In this study, we found that downregulation of PPP2R2A could promote A549 cell proliferation and anlotinib resistance. Significantly, miR-136-5p could promote A549 cell proliferation and anlotinib resistance via downregulation of PPP2R2A. Collectively, exosomal miR-136-5p functionally promoted cell proliferation and anlotinib resistance by targeting PPP2R2A after being delivered from anlotinib-resistant NSCLC cells to anlotinib-sensitive NSCLC cells.

One miRNA can regulate several mRNAs at the same time.[40] Chen et al reported that overexpression of miR-136 could promote gastric cancer cell proliferation via activation of Akt signaling by targeting PTEN.[15] Shen et al found that miR-136 could promote the NSCLC cell proliferation via activation of ERK signaling by targeting PPP2R2A.[16] Thus, miR-136 may regulate cancer progression via targeting different genes (such as PTEN and PPP2R2A). In addition, ERK and Akt signaling pathways are usually associated with proliferation and drug resistance of human cancer cells, including NSCLC cells.[41–44] Zeng et al reported that miR-222 inhibited the cisplatin sensitivity in bladder cancer cells via activation of Akt signaling by targeting PPP2R2A.[45] Consistent with previous studies, our data indicated that exosomal miR-136-5p promoted NSCLC cell proliferation and anlotinib resistance by targeting PPP2R2A and activation of Akt signaling pathway.

Conclusion

In this study, we found that anlotinib-resistant NSCLC cell-derived exosomal miR-136-5p could promote NSCLC cell proliferation and anlotinib resistance by targeting PPP2R2A. Meanwhile, exosomal miR-136-5p antagomir from anlotinib-resistant NSCLC cells could functionally restore the anlotinib response in NSCLC cells. Therefore, miR-136-5p may act as a potential biomarker for anlotinib response in NSCLC.

Data Sharing Statement

The datasets used and/or analyzed during the current study are available from the corresponding author on reasonable request.

Ethics Approval

All animal procedures were approved by the ethics committee of the Affiliated Lianyungang Hospital of Xuzhou Medical University.

Disclosure

The authors declare that they have no conflicts of interest for this work.

References

1. Bai Y, Liu X, Qi X, et al. PDIA6 modulates apoptosis and autophagy of non-small cell lung cancer cells via the MAP4K1/JNK signaling pathway. *EBioMedicine*. 2019;42:311–325. doi:10.1016/j.ebiom.2019.03.045

2. Feng H, Ge F, Du L, Zhang Z, Liu D. MiR-34b-3p represses cell proliferation, cell cycle progression and cell apoptosis in non-small-cell lung cancer (NSCLC) by targeting CDK4. *J Cell Mol Med*. 2019;23(8):5282–5291. doi:10.1111/jcmm.14404

3. Ridge CA, McErlean AM, Ginsberg MS. Epidemiology of lung cancer. *Semin Intervent Radiol*. 2013;30(2):93–98. doi:10.1055/s-0033-1342949

4. Herbst RS, Heymach JV, Lippman SM. Lung cancer. *N Engl J Med*. 2008;359(13):1367–1380. doi:10.1056/NEJMra0802714

5. Liang L, Hui K, Hu C, et al. Autophagy inhibition potentiates the anti-angiogenic property of multikinase inhibitor anlotinib through JAK2/STAT3/VEGFA signaling in non-small cell lung cancer cells. *J Exp Clin Cancer Res*. 2019;38(1):71. doi:10.1186/s13046-019-1093-3

6. Han B, Li K, Wang Q, et al. Effect of anlotinib as a third-line or further treatment on overall survival of patients with advanced non-small cell lung cancer: the ALTER 0303 Phase 3 randomized clinical trial. *JAMA Oncol*. 2018;4(11):1569–1575. doi:10.1001/jamaoncol.2018.3039

7. Théry C. Exosomes: secreted vesicles and intercellular communications. *F1000 Biol Rep*. 2011;3:15. doi:10.3410/B3-15

8. Zhang L, Yu D. Exosomes in cancer development, metastasis, and immunity. *Biochim Biophys Acta Rev Cancer*. 2019;1871(2):455–468. doi:10.1016/j.bbcan.2019.04.004

9. Yu X, Odenthal M, Fries JW. Exosomes as miRNA carriers: formation-function-future. *Int J Mol Sci*. 2016;17(12):12. doi:10.3390/ijms17122028

10. Li S, Li Y, Chen B, et al. exoRBase: a database of circRNA, lncRNA and mRNA in human blood exosomes. *Nucleic Acids Res*. 2018;46(D1):D106–d112. doi:10.1093/nar/gkx891

11. Raposo G, Stoorvogel W. Extracellular vesicles: exosomes, micro-vesicles, and friends. *J Cell Biol*. 2013;200(4):373–383. doi:10.1083/jcb.201211138

12. Ganju A, Khan S, Hafeez BB, et al. miRNA nanotherapeutics for cancer. *Drug Discov Today*. 2017;22(2):424–432. doi:10.1016/j.drudis.2016.10.014

13. Ji Q, Xu X, Song Q, et al. miR-223-3p inhibits human osteosarcoma metastasis and progression by directly targeting CDH6. *Mol Ther*. 2018;26(5):1299–1312. doi:10.1016/j.ymthe.2018.03.009

14. Bushati N, Cohen SM. microRNA functions. *Annu Rev Cell Dev Biol*. 2007;23(1):175–205. doi:10.1146/annurev.cellbio.23.090506.123406

15. Chen X, Huang Z, Chen R. Microrna-136 promotes proliferation and invasion ingastric cancer cells through Pten/Akt/P-Akt signaling pathway. *Oncol Lett*. 2018;15(4):4683–4689.

16. Shen S, Yue H, Li Y, et al. Upregulation of miR-136 in human non-small cell lung cancer cells promotes Erk1/2 activation by target-ing PPP2R2A. *Tumour Biol*. 2014;35(1):631–640. doi:10.1007/s13277-013-1087-2

17. Jayaraj R, Nayagam SG, Kar A, et al. Clinical theragnostic relation-ship between drug-resistance specific miRNA expressions, che-motherapeutic resistance, and sensitivity in breast cancer: a systematic review and meta-analysis. *Cells*. 2019;8(10):10. doi:10.3390/cells8101250

18. Wu J, Mao X, Cai T, Luo J, Wei L. KOBAS server: a web-based platform for automated annotation and pathway identification. *Nucleic Acids Res*. 2006;34(Web Server):W720–W724. doi:10.1093/nar/gkl167

19. Zhang J, Li S, Li L, et al. Exosome and exosomal microRNA: trafficking, sorting, and function. *Genomics Proteomics Bioinformatics*. 2015;13(1):17–24. doi:10.1016/j.gpb.2015.02.001

20. Wang X, Xu J, Chen J, et al. IL-22 confers EGFR-TKI resistance in NSCLC via the AKT and ERK signaling pathways. *Front Oncol*. 2019;9:1167. doi:10.3389/fonc.2019.01167

21. Sun CY, Zhu Y, Li XF, et al. Scutellarin increases cisplatin-induced apoptosis and autophagy to overcome cisplatin resistance in non-small cell lung cancer via ERK/p53 and c-met/AKT signaling pathways. *Front Pharmacol*. 2018;9:92. doi:10.3389/fphar.2018.00092

22. Zhang W, Song C, Ren X. Circ_0003998 regulates the progression and docetaxel sensitivity of DTX-resistant non-small cell lung cancer cells by the miR-136-5p/CORO1C axis. *Technol Cancer Res Treat*. 2021;20:1533033821990040.

23. Grootjans W, de Geus-oei LF, Troost EG, et al. PET in the manage-ment of locally advanced and metastatic NSCLC. *Nat Rev Clin Oncol*. 2015;12(7):395–407. doi:10.1038/nrclinonc.2015.75

24. Doval DC, Desai CJ, Sahoo TP. Molecularly targeted therapies in non-small cell lung cancer: the evolving role of tyrosine kinase inhibitors. *Indian J Cancer*. 2019;56(5):S23–s30. doi:10.4103/ijc.IJC_449_19

25. Wang Y, Wen L, Zhao SH, et al. FoxM1 expression is significantly associated with cisplatin-based chemotherapy resistance and poor prognosis in advanced non-small cell lung cancer patients. *Lung Cancer*. 2013;79(2):173–179. doi:10.1016/j.lungcan.2012.10.019

26. Han B, Li K, Zhao Y, et al. Anlotinib as a third-line therapy in patients with refractory advanced non-small-cell lung cancer: a multicentre, randomised Phase II trial (ALTER0302). *Br J Cancer*. 2018;118(5):654–661. doi:10.1038/bjc.2017.478

27. Lobb RJ, van Amerongen R, Wiegmans A, et al. Exosomes derived from mesenchymal non-small cell lung cancer cells promote chemoresistance. *Int J Cancer*. 2017;141(3):614–620. doi:10.1002/ijc.30752

28. Santos JC, Lima NDS, Sarian LO, et al. Exosome-mediated breast cancer chemoresistance via miR-155 transfer. *Sci Rep*. 2018;8(1):829.

29. Zhang C, Zhang K, Huang F, et al. Exosomes, the message transpor-ters in vascular calcification. *J Cell Mol Med*. 2018;22(9):4024–4033. doi:10.1111/jcmm.13692

30. Melo SA, Sugimoto H, O'Connell JT, et al. Cancer exosomes per-form cell-independent microRNA biogenesis and promote tumorigenesis. *Cancer Cell*. 2014;26(5):707–721. doi:10.1016/j.ccell.2014.09.005

31. Fan J, Xu G, Chang Z, Zhu L, Yao J. miR-210 transferred by lung cancer cell-derived exosomes may act as proangiogenic factor in cancer-associated fibroblasts by modulating JAK2/STAT3 pathway. *Clin Sci (Lond)*. 2020;134(7):807–825. doi:10.1042/CS20200039

32. Kim DH, Park S, Kim H, et al. Tumor-derived exosomal miR-619-5p promotes tumor angiogenesis and metastasis through the inhibition of RCAN1.4. *Cancer Lett*. 2020;475:2–13. doi:10.1016/j.canlet.2020.01.023

33. Yang Z, Zhao N, Cui J, et al. Exosomes derived from cancer stem cells of gemcitabine-resistant pancreatic cancer cells enhance drug resistance by delivering miR-210. *Cell Oncol*. 2020;43(1):123–136. doi:10.1007/s13402-019-00476-6

34. Sousa D, Lima RT, Vasconcelos MH. Intercellular transfer of cancer drug resistance traits by extracellular vesicles. *Trends Mol Med*. 2015;21(10):595–608. doi:10.1016/j.molmed.2015.08.002

35. Qiu Z, Fa P, Liu T, et al. A genome-wide pooled shRNA screen identifies PPP2R2A as a predictive biomarker for the response to ATR and CHK1 inhibitors. *Cancer Res*. 2020;80(16):3305–3318. doi:10.1158/0008-5472.CAN-20-0057

36. Li R, Li J, Yang H, et al. Hepsin promotes epithelial-mesenchymal transition and cell invasion through the miR-222/PPP2R2A/AKT axis in prostate cancer. *Onco Targets Ther*. 2020;13:12141–12149. doi:10.2147/OTT.S268025

37. Yu WC, Chen HH, Qu YY, et al. MicroRNA-221 promotes cisplatin resistance in osteosarcoma cells by targeting PPP2R2A. *Biosci Rep*. 2019;39(7):BSR20190198.. doi:10.1042/BSR20190198.

38. Zhang CF, Kang K, Li XM, Xie BD. MicroRNA-136 promotes vascular muscle cell proliferation through the ERK1/2 pathway by targeting PPP2R2A in atherosclerosis. *Curr Vasc Pharmacol*. 2015;13(3):405–412. doi:10.2174/1570161112666141118094612

39. Zhang D, Wang J, Wang Z, et al. miR-136 modulates TGF-β1-induced proliferation arrest by targeting PPP2R2A in keratino-cytes. *Biomed Res Int*. 2015;2015:453518.

40. Vasu MM, Sumitha PS, Rahna P, Thanseem I, Anitha A. microRNAs in autism spectrum disorders. *Curr Pharm Des*. 2019;25(41):4368–4378. doi:10.2174/1381612825666191105120901

41. Ye L, Pu C, Tang J, et al. Transmembrane-4 L-six family member-1 (TM4SF1) promotes non-small cell lung cancer proliferation, inva-sion and chemo-resistance through regulating the DDR1/Akt/ERK-mTOR axis. *Respir Res*. 2019;20(1):106. doi:10.1186/s12931-019-1071-5

42. Wu Z, Xu B, Yu Z, et al. Trifolium flavonoids overcome gefitinib resistance of non-small-cell lung cancer cell by suppressing ERK and STAT3 signaling pathways. *Biomed Res Int*. 2020;2020:2491304. doi:10.1155/2020/2491304

43. Wang F, Meng F, Wong SCC, et al. Combination therapy of gefitinib and miR-30a-5p may overcome acquired drug resistance through regulating the PI3K/AKT pathway in non-small cell lung cancer. *Ther Adv Respir Dis*. 2020;14:1753466620915156. doi:10.1177/1753466620915156

44. Liu N, Zhu M, Linhai Y, et al. Increasing HER2 α2,6 sialylation facilitates gastric cancer progression and resistance via the Akt and ERK pathways. *Oncol Rep*. 2018;40(5):2997–3005.

45. Zeng LP, Hu ZM, Li K, Xia K. miR-222 attenuates cisplatin-induced cell death by targeting the PPP2R2A/Akt/mTOR axis in bladder cancer cells. *J Cell Mol Med*. 2016;20(3):559–567. doi:10.1111/jcmm.12760